



Back-Stepping Integral Sliding Mode Control with Iterative Learning Control Algorithm for Quadrotor UAVs

Davood Allahverdy¹ · Ahmad Fakharian² · Mohammad Bagher Menhaj³

Received: 14 May 2019 / Revised: 9 July 2019 / Accepted: 5 August 2019 / Published online: 29 August 2019
© The Korean Institute of Electrical Engineers 2019

Abstract

In this study, back-stepping integral sliding mode control (BISMC) with iterative learning control (ILC) algorithm are presented for nonlinear translational and rotational dynamics of the Quadrotor UAVs. The proposed controller (BISMC) can track desired trajectories and (ILC) is responsible for inclining the accuracy and robustness of the control strategy. In order to prove the stability of the closed loop system, Lyapunov theorem is used. The simulation results indicate that the proposed control strategy has high accuracy, suitable robustness, disturbance rejection, good trajectory tracking and fast transient responses for the Quadrotor UAVs despite the uncertainties and external disturbances.

Keywords Back-stepping integral sliding mode control · Quadrotor UAVs · Iterative learning control · Disturbance rejection

1 Introduction

Nowadays, Quadrotor UAV plays a significant role in people life and researchers have paid more attention for designing better control strategy for it. Due to the Quadrotor UAVs features such as speed, small size and environmentally friendly, it has been applying for weather monitoring, relief and rescue operation and military purposes, etc. The dynamic of the Quadrotor UAVs is highly coupled, nonlinear and under actuated, therefore it's very difficult to design a robust controller despite the external disturbances and uncertainties. One more fact should be taken into consideration is that

the Quadrotor UAVs is affected by aerodynamic effects and inertial torque during the flight pass.

It's well known that sliding mode control (SMC) is a nonlinear control strategy which could cope with the uncertainties and external disturbances on sliding surface [1–5] and this powerful method repeatedly was applied for the Quadrotor UAVs. In [6], an adaptive sliding mode control by feedback linearization were used for a Quadrotor helicopter. In [7, 8], a new fuzzy integral sliding surface was designed for improving the stability of the nonlinear system. In [9], a finite-time control algorithm based on SMC was improved for altitude control of the Quadrotor UAVs and multi variable finite-time control were used in [10, 11]. In order to cope with the uncertainties, an adaptive sliding mode control was designed for the Quadrotor UAVs. Additional references about SMC can be found in [12, 13]. In [14], a Mixed H₂/H_∞ Controller based on LMI based Approach is used. The mentioned control strategies can improve the robustness of the system.

In the recent years, combination of back-stepping and sliding mode control was used for controlling the altitude and the position of the Quadrotor UAVs which back-stepping is used to track the desired trajectory [15] and SMC is responsible for inclining the robustness of the system [16, 17]. In [18], back-stepping and sliding mode techniques were applied to distributed secondary control of micro Quadrotor UAVs. A new fuzzy back-stepping sliding mode control was

✉ Ahmad Fakharian
ahmad.fakharian@qiau.ac.ir

Davood Allahverdy
davoodallahverdi72@gmail.com

Mohammad Bagher Menhaj
menhaj@aut.ac.ir

¹ Science and Research Branch, Islamic Azad University, Tehran, Iran

² Faculty of Electrical, Biomedical and Mechatronics Engineering, Qazvin Branch, Islamic Azad University, Qazvin, Iran

³ Department of Electrical Engineering, Amirkabir University of Technology, Tehran, Iran

provided for the under-actuated Quadrotor UAVs in [19]. In [20], an adaptive back-stepping control method was designed and analyzed for fault-tolerant of the nonlinear system. In [21], despite of unmodeled dynamics, a new fuzzy adaptive back-stepping controller was used. In [22], a multi variable sliding mode with back-stepping controller based on disturbance observe was presented. A hybrid method based on fuzzy integral back-stepping controller was designed for hovering the Quadrotor [23]. In [24], combination of neural network and back-stepping was designed for helicopter.

Iterative learning control is formulated based on its previous experiments and repeatedly performed for a same task in order to increase the accuracy and the robustness against the uncertainties and external disturbances. In [25], a novel fuzzy PID-type iterative learning control was applied for the Quadrotor UAVs and in order to account with the unmodeled dynamic and systematic error, an adaptive tracking control with iterative learning control were used in [26]. In [27], an online PID-iterative learning control with switching gain was used for circular trajectory motion in three dimensions. For the precise Quadrotor UAVs trajectory tracking, optimization based on iterative learning control was used [28]. In [29], for accurate control of a team of Quadrotors, a distributed iterative learning control was used. According to the mentioned references, iterative learning control can incline the accuracy of the system and reject the disturbances by using simple update rules.

The main novelty of this paper is designing back-stepping integral sliding mode control with iterative learning control for the Quadrotor UAVs. On the other hand, the back-stepping is responsible for tracking the desired trajectory and the highly coupled feature of under-actuated of the dynamic are sought by virtual controller. Next, the integral sliding mode controller is designed and analyzed for coping with the uncertainties and external disturbances. In addition, in order to improve the accuracy of the tracking, iterative learning control is designed according to previous experiments which is resulted in better tracking, accuracy and robustness and lower errors of states.

The remaining part of this paper are organized as follow: Sect. 2 presents the Quadrotor UAVs dynamics. The back-stepping integral sliding mode control using Lyapunov theory are given in Sect. 3. Designing the iterative learning control is presented in Sect. 4. Simulation results are presented in Sect. 5 and finally, Sect. 6 Concludes the paper.

2 Quadrotor UAVs Model

In this paper, the model for dynamic of the Quadrotor UAVs is considered from [30], which is nonlinear, strongly coupled and under actuated. The Quadrotor UAVs structure is shown in Fig. 1 which consists of four rotors. In this structure two types of coordinate system such as earth coordinate $\xi = [x,$

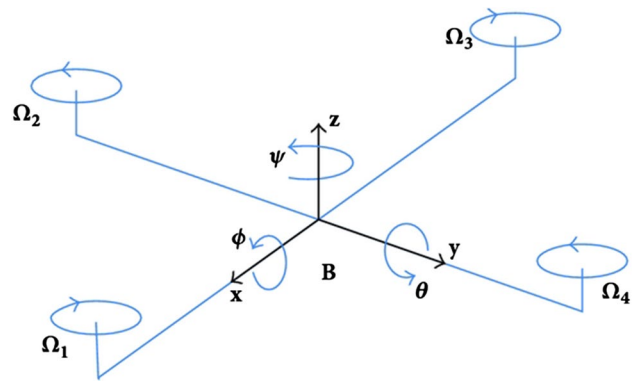


Fig. 1 Quadrotor UAVs Structure

$y, z]$ and body coordinate $\eta = [\phi, \theta, \Psi]$ were defined. The $[x, y, z]$ denote the position of the Quadrotor UAVs and $[\phi, \theta, \Psi]$ refer to roll angle, pitch angle and yaw angle which could control the altitude of the Quadrotor UAVs. It should be mentioned that the movement of the Quadrotor UAVs in different directions are achieved based on the thrust generated by adjusting the rotational speeds of the four rotors. According to [30], the translational and the rotational dynamic model for the Quadrotor UAVs can be defined as follow:

$$\begin{aligned} \tau &= J\dot{\omega} + \omega(J\omega + J_r\Omega_r e_3) + d_\tau \\ m\dot{v} &= RT - mge_3 - d_T \end{aligned} \tag{1}$$

where ω is the angular velocity vector, τ refers to the torque vector for the three axes, J denotes the inertia tensor, $\Omega_r = \Omega_1 - \Omega_2 + \Omega_3 - \Omega_4$ is the component torques in the three directions, R is the rotation matrix, J_r describes the moment of the rotor inertia, T is the force vector, d_τ and d_T are the disturbance vectors for the translational and rotational subsystems respectively.

Based on Eq. (1), equations of the motion in each axes are described as follow [28]:

$$\ddot{x} = (\sin \theta \cos \phi \cos \Psi + \sin \phi \sin \Psi) \left(\frac{b}{m} \right) u_1 - \frac{d_x}{m} \tag{2}$$

$$\ddot{y} = (\cos \phi \sin \theta \cos \Psi - \sin \phi \sin \Psi) \left(\frac{b}{m} \right) u_1 - \frac{d_y}{m} \tag{3}$$

$$\ddot{z} = -g + \cos \theta \cos \phi \left(\frac{b}{m} \right) u_1 - \frac{d_z}{m} \tag{4}$$

$$\ddot{\phi} = \dot{\theta} \dot{\Psi} \frac{I_y - I_z}{I_y} + \dot{\theta} \Omega_r \frac{J_r}{I_x} + \frac{Lb}{I_x} u_2 - \frac{d_\phi}{I_x} \tag{5}$$

$$\ddot{\theta} = \dot{\phi} \dot{\Psi} \frac{I_z - I_x}{I_y} + \dot{\phi} \Omega_r \frac{J_r}{I_y} + \frac{Lb}{I_y} u_3 - \frac{d_\theta}{I_y} \tag{6}$$

$$\ddot{\Psi} = \dot{\phi}\dot{\theta} \frac{I_x - I_y}{I_z} + \frac{d}{I_z}u_4 - \frac{d_{\Psi}}{I_z} \tag{7}$$

where L is the Quadrotor UAVs arm length, d is the drag coefficient, b refers to the thrust coefficient, m denote the total Quadrotor UAVs mass and $I_{x,y,z}$ are the moments of inertia about x, y, z axes. The parameters of the motion equations are defined in Table 1.

The relationship between the control inputs and the rotors speed in each axes is described as:

$$U = \begin{bmatrix} u_1 \\ u_2 \\ u_3 \\ u_4 \end{bmatrix} = \begin{bmatrix} 1 & 1 & 1 & 1 \\ 0 & -1 & 0 & 1 \\ 1 & 0 & -1 & 0 \\ 1 & -1 & 1 & -1 \end{bmatrix} \begin{bmatrix} \Omega_1^2 \\ \Omega_2^2 \\ \Omega_3^2 \\ \Omega_4^2 \end{bmatrix} \tag{8}$$

It should be mentioned that the translational dynamic is controlled by u_1 and the rotational dynamic is related to u_2, u_3 and u_4 .

In order to design the controller, the state variables are selected as follow:

$$X = [x, y, z, \phi, \theta, \Psi, \dot{x}, \dot{y}, \dot{z}, \dot{\phi}, \dot{\theta}, \dot{\Psi}] \tag{9}$$

Then according to Eqs. (2–7), a state space representation for Quadrotor UAVs can be achieved as:

$$\dot{X} = \begin{bmatrix} x_7 \\ x_8 \\ x_9 \\ x_{10} \\ x_{11} \\ x_{12}(\sin x_5 \cos x_4 \cos x_6 + \sin x_4 \sin x_6) \left(\frac{b}{m}\right)u_1 - \frac{d_x}{m} \\ (\cos x_4 \sin x_5 \cos x_6 - \sin x_4 \sin x_6) \left(\frac{b}{m}\right)u_1 - \frac{d_y}{m} \\ -g + \cos x_5 \cos x_4 \left(\frac{b}{m}\right)u_1 - \frac{d_z}{m} \\ x_{11}x_{12} \frac{I_y - I_z}{I_x} + x_{11}\Omega_r \frac{J_r}{I_x} + \frac{Lb}{I_x}u_2 - \frac{d_{\phi}}{I_x} \\ x_{10}x_{12} \frac{I_z - I_x}{I_y} + x_{10}\Omega_r \frac{J_r}{I_y} + \frac{Lb}{I_y}u_3 - \frac{d_{\theta}}{I_y} \\ x_{11}x_{12} \frac{I_x - I_y}{I_z} + \frac{d}{I_z}u_4 - \frac{d_{\Psi}}{I_z} \end{bmatrix}$$

It's crystal clear that the body coordinate angles and their time derivation don't depend on the earth coordinate states and the whole of the dynamic can be decoupled into two subsystems: the angular rotations and the linear translation. The control system schematic diagram for this approach is shown in Fig. 2.

In this section the desired trajectories are calculated by considering Eqs. (2) and (3) which extremely depend on the roll and pitch angles and the desired positions are transformed into commands of the roll angle and the pitch angle:

$$\ddot{x}_d = (\sin x_{5d} \cos x_{4d} \cos x_{6d} + \sin x_{4d} \sin x_{6d}) \left(\frac{b}{m}\right)u_1 \tag{10}$$

$$\ddot{y}_d = (\cos x_{4d} \sin x_{5d} \cos x_{6d} + \sin x_{4d} \sin x_{6d}) \left(\frac{b}{m}\right)u_1 \tag{11}$$

where \ddot{x}_d and \ddot{y}_d can be approximated by $\ddot{x}_d = k_x e_x$ and $\ddot{y}_d = k_y e_y$ where k_x and k_y are positive constants. The desired commands for both roll and pitch angles are designed as follow:

$$x_{4d} = \cos^{-1} \left(\frac{mk_x e_x}{bu_1 \sin x_{5d} \cos x_{6d}} - \frac{\sin x_{4d} \sin x_{6d}}{\sin x_{5d} \cos x_{6d}} \right) \tag{12}$$

Table 1 Parameters of quadrotor UAVs dynamic

Parameters	Value	Unit
L	0.232	m
b	3.13×10^{-5}	$n \text{ s}^2$
d	7.5×10^{-7}	$m \text{ s}^2$
m	0.52	kg
I_x	6.228×10^{-3}	kg m^2
I_y	6.228×10^{-3}	kg m^2
I_z	1.121×10^{-2}	kg m^2
J_r	6×10^{-5}	kg m^2
Ω_{\max}	297	rad/s

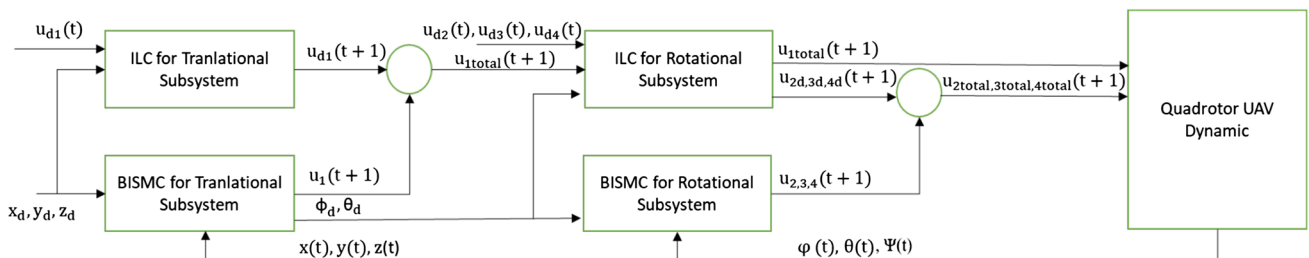


Fig. 2 The control system schematic diagram

$$x_{5d} = \sin^{-1} \left(\frac{mk_y e_y}{bu_1 \cos x_{4d} \cos x_{6d}} + \frac{\sin x_{4d} \sin x_{6d}}{\cos x_{4d} \cos x_{6d}} \right) \quad (13)$$

It can be concluded from the analysis of Eqs. (2) and (3) that the position of the Quadrotor UAVs indirectly are controlled by φ , θ which are adjusted by u_2 and u_3 . In addition, the altitude of the Quadrotor UAVs and the yaw angle are directly controlled by u_1 and u_4 respectively.

3 BISM Design for Translational Subsystem

Define $z_3 = x_3 - x_{3d}$ as error of the altitude. The time derivation of z_3 will be $\dot{z}_3 = \dot{x}_3 - \dot{x}_{3d}$.

According to stability theory (Lyapunov), a positive candidate function is defined as $v_1 = \frac{1}{2}z_3^2$ and the time derivation of v_1 will be $\dot{v}_1 = z_3\dot{z}_3$.

$$\dot{v}_1 = z_3(\dot{x}_3 - \dot{x}_{3d}) \quad (14)$$

Define $z_6 = \dot{x}_3 - a_1$, where a_1 is a virtual control input. Then \dot{v}_1 is written as:

$$\dot{v}_1 = z_3z_6 + z_3(a_1 - \dot{x}_{3d}). \quad (15)$$

In order to make sure that Eq. (15) is stable, a_1 is implemented as:

$$a_1 = \dot{x}_{3d} - c_1z_3 \quad (16)$$

where c_1 is a non-zero positive constant. In addition, the time derivation of v_1 can be computed as:

$$\dot{v}_1 = z_3z_6 + z_3(\dot{x}_{3d} - c_1z_3 - \dot{x}_{3d}) = -c_1z_3^2 + z_3z_6. \quad (17)$$

The integral sliding mode surface for the altitude state is considered as follow:

$$s_1 = z_6 + k_1 \int z_3. \quad (18)$$

By considering the switching law as:

$$\dot{s}_1 = -\varepsilon s_1 - \text{sgn}(s_1) \quad (19)$$

where ε is a positive constant and the time derivation of s_1 is calculated as follow:

$$\dot{z}_6 + k_1z_3 = -\varepsilon s_1 - \text{sgn}(s_1). \quad (20)$$

By combination of the Lyapunov theory and the integral sliding mode, the control input u_1 is designed as follow:

$$u_1 = \frac{m}{\cos x_5 \cos x_4 b} \left[-(k_1 + c_1)z_3 + g - \varepsilon s_1 - \text{sgn}(s_1) + \dot{x}_{6d} + \frac{d_z}{m} \right]. \quad (21)$$

For the stability analysis, a positive Lyapunov function is selected as:

$$v_2 = \frac{1}{2}v_1^2 + \frac{1}{2}s_1^2. \quad (22)$$

The time derivation of Eq. (22) is calculated as:

$$\dot{v}_2 = v_1\dot{v}_1 + s_1\dot{s}_1. \quad (23)$$

And

$$\dot{v}_2 = v_1\dot{v}_1 + s_1 \left(-g + \cos x_5 \cos x_4 \left(\frac{b}{m} \right) u_1 - \frac{d_z}{m} \right). \quad (24)$$

By substituting (21) into (24), the necessary condition of Lyapunov theorem verified ($\dot{v}_2 < 0$).

3.1 BISM Design for Rotational Subsystem

By defining $z_4 = x_4 - x_{4d}$ as error of the roll angle, the time derivation of z_4 will be $\dot{z}_4 = \dot{x}_4 - \dot{x}_{4d}$.

The stability of the roll angle state is analyzed by Lyapunov theory with defining a positive definite function as $v_3 = \frac{1}{2}z_4^2$ and the time derivation of v_3 will be $\dot{v}_3 = z_4\dot{z}_4$. Then:

$$\dot{v}_3 = z_4(\dot{x}_4 - \dot{x}_{4d}). \quad (25)$$

Define $z_{10} = \dot{x}_4 - a_2$, where a_2 is virtual control input. Then \dot{v}_3 can be concluded:

$$\dot{v}_3 = z_4z_{10} + z_4(a_2 - \dot{x}_{4d}). \quad (26)$$

In order to make sure that Eq. (26) is stable, a_2 is defined as:

$$a_2 = \dot{x}_{4d} - c_2z_4, \quad (27)$$

where c_2 is a non-zero positive constant. Furthermore, the time derivation of v_3 can be achieved as:

$$\dot{v}_3 = z_4z_{10} + z_4(\dot{x}_{4d} - c_2z_4 - \dot{x}_{4d}) = -c_2z_4^2 + z_4z_{10}. \quad (28)$$

The integral sliding mode surface for the roll angle state is defined as follow:

$$s_2 = z_{10} + k_2 \int z_4 \quad (29)$$

Now consider the reaching law as:

$$\dot{s}_2 = -\varepsilon s_2 - \text{sgn}(s_2) \quad (30)$$

where ε is a positive constant. By the time derivation of Eq. (29):

$$\dot{z}_{10} + k_2z_4 = -\varepsilon s_2 = \text{sgn}(s_2) \quad (31)$$

According to Eqs. (28)–(31), the control input u_2 is designed as follow:

$$u_2 = \frac{I_x}{Lb} \left[-(k_2 + c_2)z_4 - \varepsilon s_2 - \text{sgn}(s_2) + \dot{x}_{10d} + \frac{d_\varphi}{I_x} - x_{11}\Omega_r \frac{J_r}{I_x} - x_{11}x_{12} \frac{I_y - I_z}{I_y} \right]. \quad (32)$$

For examining the stability, a positive Lyapunov function is defined as:

$$v_4 = \frac{1}{2}v_3^2 + \frac{1}{2}s_2^2. \quad (33)$$

The time derivation of Eq. (33) is calculated as follow:

$$\dot{v}_4 = v_3 \dot{v}_3 + s_2 \dot{s}_2. \tag{34}$$

And

$$\dot{v}_4 = v_3 \dot{v}_3 + s_1 \left(x_{11} x_{12} \frac{I_y - I_z}{I_y} + x_{11} \Omega_r \frac{J_r}{I_x} + \frac{Lb}{I_x} u_2 - \frac{d_\varphi}{I_x} \right). \tag{35}$$

By replacing (32) into (35), the necessary condition of Lyapunov theorem is verified ($\dot{v}_4 < 0$).

It should be mentioned that the next steps are similar with u_2 , so u_3 and u_4 can be achieved in the same way:

$$u_3 = \frac{I_y}{Lb} \left[-(k_3 + c_3)z_5 - \varepsilon s_3 - \text{sgn}(s_3) + \dot{x}_{12d} + \frac{d_\theta}{I_y} - x_{10} \Omega_r \frac{J_r}{I_y} - x_{10} x_{12} \frac{I_z - I_x}{I_y} \right] \tag{36}$$

$$u_4 = \frac{I_z}{d} \left[-(k_4 + c_3)z_6 - \varepsilon s_4 - \text{sgn}(s_4) + \dot{x}_{12d} + \frac{d_\varphi}{I_z} - x_{11} x_{12} \frac{I_x - I_y}{I_z} \right] \tag{37}$$

4 Iterative Learning Control

In this section, the iterative learning control (ILC) is designed and analyzed for the system for precise tracking of the desired trajectory. ILC is based on previous experiments so that in each iteration the recorded trajectories are analyzed in order to calculate the next commands as control inputs for better converging the actual values to reference trajectories. Standard iterative learning control scheme is shown in Fig. 3. On the other hand, ILC is able to cope with repetitive disturbance or systematic error in the model. The formulation of the iterative learning control is inspired from [31].

At first, the states and the relative control inputs are considered separately in two vectors as follow:

$$U = [U_1 U_2 U_3 U_4]^T$$

$$X = [X_9 X_{10} X_{11} X_{12}]^T, \tag{38}$$

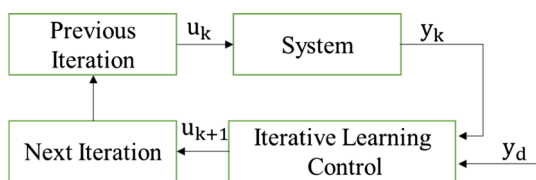


Fig. 3 Iterative learning control scheme

where

$$\begin{bmatrix} X_9 \\ X_{10} \\ X_{11} \\ X_{12} \end{bmatrix} = \begin{bmatrix} -g + \cos x_5 \cos x_4 \left(\frac{b}{m} \right) u_1 - \frac{d_z}{m} \\ x_{11} x_{12} \frac{I_y - I_z}{I_y} + x_{11} \Omega_r \frac{J_r}{I_x} + \frac{Lb}{I_x} u_2 - \frac{d_\varphi}{I_x} \\ x_{10} x_{12} \frac{I_z - I_x}{I_y} + x_{10} \Omega_r \frac{J_r}{I_y} + \frac{Lb}{I_y} u_3 - \frac{d_\theta}{I_y} \\ x_{11} x_{12} \frac{I_x - I_y}{I_z} + \frac{d}{I_z} u_4 - \frac{d_\psi}{I_z} \end{bmatrix}. \tag{39}$$

Due to the perfect model (39), the desired trajectory can be tracked using the back-stepping integral sliding mode controller as:

$$X_{ref} = f(U_{BISMIC}). \tag{40}$$

The main idea of the ILC is not approximating the uncertainties of the model but is calculating the commands input as unknown disturbance input U_d . That is to combine with U_{BISMIC} for better tracking the desired trajectory. The total control input is designed as follow:

$$U_{total} = U_{BISMIC} + U_d$$

$$\dot{X}_j = f(U_{total}) \tag{41}$$

$$\dot{X}_j = f(U_{BISMIC} + U_d).$$

The update law for estimation of the next command for the unknown disturbance input U_d is described as:

$$U_{d,j+1} = U_{d,j} - F^T K \delta_j \tag{42}$$

where K is a positive matrix and F is a matrix which is achieved according to Eq. (39) along the desired trajectories by linear time varying method as follow:

$$F = \begin{bmatrix} \frac{dX_9}{dU_1} & \dots & \frac{dX_9}{dU_4} \\ \vdots & \ddots & \vdots \\ \frac{dX_{12}}{dU_1} & \dots & \frac{dX_{12}}{dU_4} \end{bmatrix}. \tag{43}$$

In addition, δ_j refers to the error vector between the desired trajectory and the actual value.

$$\delta_j = \dot{X}_j - \dot{X}_{ref} \tag{44}$$

Then Eq. (41) can be written around the ideal operating point of U_{BISMIC} .

$$\dot{X}_j = f(U_{BISMIC} + U_d) \sim f(U_{BISMIC}) + \left(\frac{d}{dU} f|_{U_{BISMIC}} \right) \cdot U_d \tag{45}$$

Finally, Eq. (44) can be achieved as function of the unknown disturbance input as:

$$\delta_j = \dot{X}_j - \dot{X}_{ref} = \left(\frac{d}{dU} f|_{U_{BISMIC}} \right) \cdot U_d = F U_d \tag{46}$$

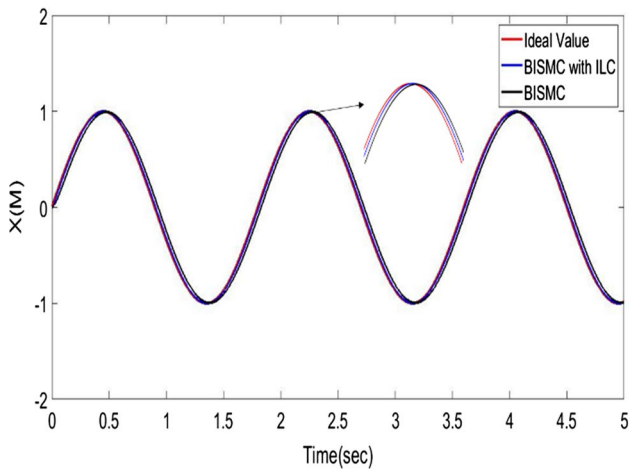


Fig. 4 Position X (M)

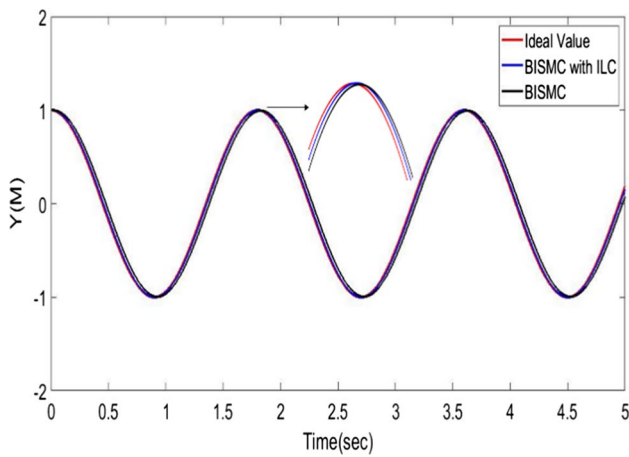


Fig. 5 Position Y (M)

5 Simulation

In this section, the effectiveness of the proposed method in comparison with only BISM is validated. The desired trajectories for x, y and z axes are selected as: $x_d = \sin\left(\frac{2\pi}{50}t\right)$, $y_d = \cos\left(\frac{2\pi}{50}t\right)$ and $z_d = 3t$ and Eqs. (10) and (11) refer to reference commands for φ and θ . The initial states are defined as $x(0) = 0$, $y(0) = 1$, $z(0) = 0$, $\varphi(0) = 0$, $\theta(0) = 0$, $\Psi(0) = -0.12$. The external disturbances are defined as follow:

$$d_x = 2 \sin t, \quad d_y = 2 \sin t, \quad d_z = 2 \sin t,$$

$$d_\varphi = 0.1 \sin\left(\frac{2\pi}{50}t\right), \quad d_\theta = 0.1 \sin\left(\frac{2\pi}{50}t\right),$$

$$d_\Psi = 0.1 \sin\left(\frac{2\pi}{50}t\right).$$

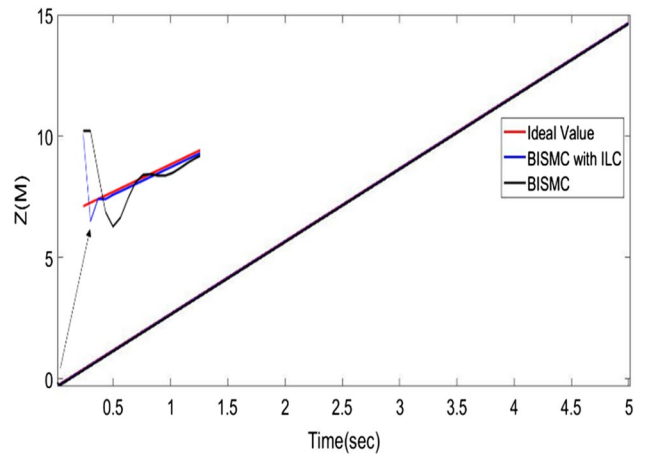


Fig. 6 Position Z (M)

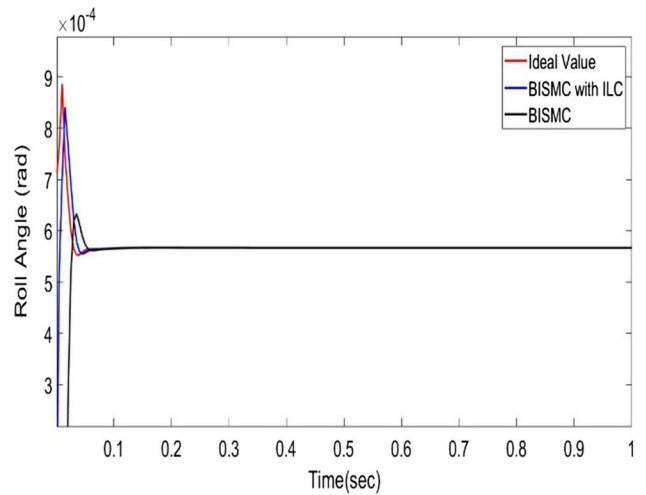


Fig. 7 Roll angle (rad)

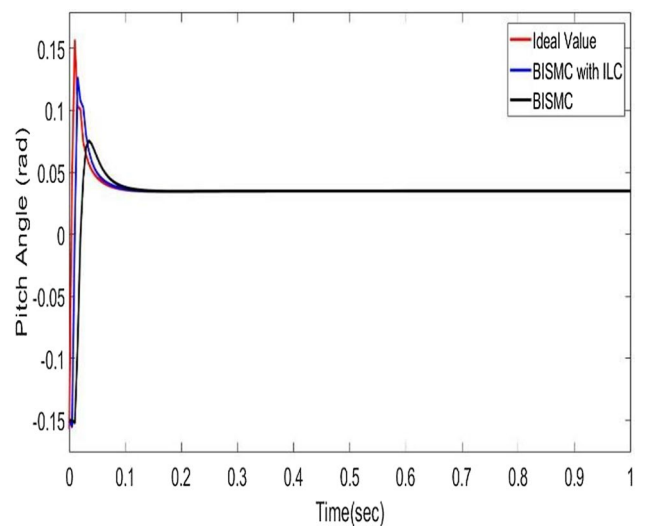


Fig. 8 Pitch angle (rad)

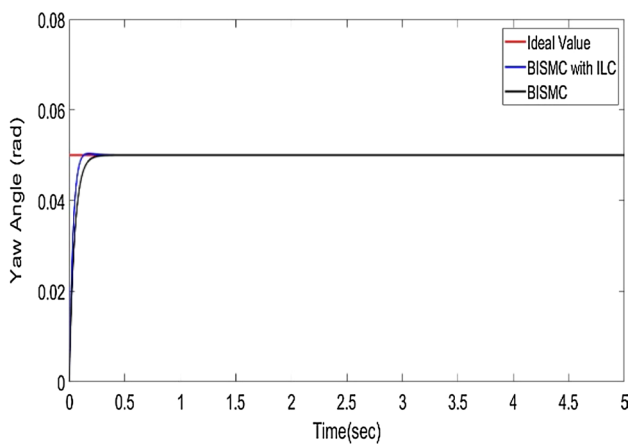


Fig. 9 Yaw angle

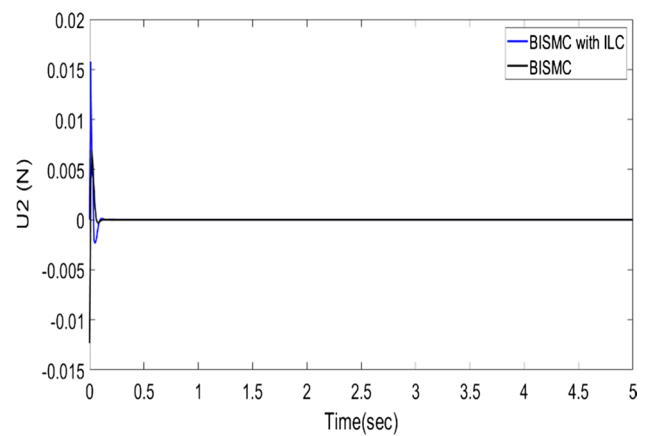


Fig. 12 Control input U_3 (N)

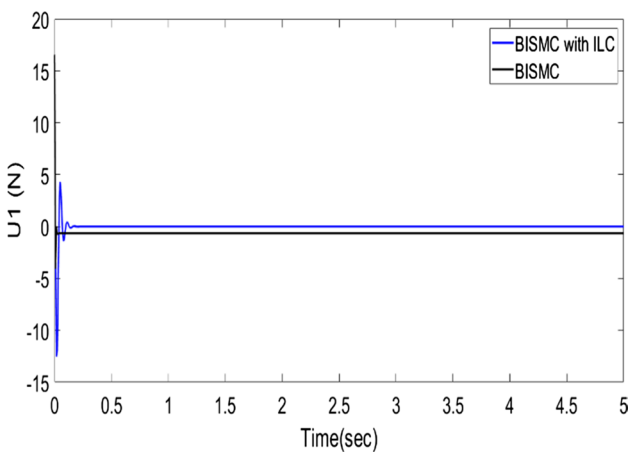


Fig. 10 Control input U_1 (N)

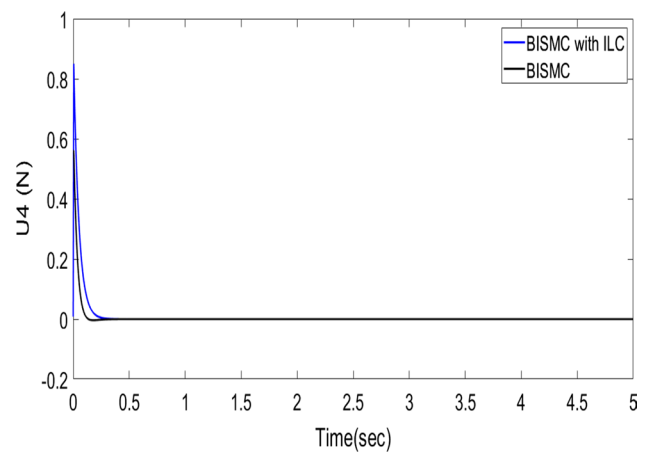


Fig. 13 Control input U_4 (N)

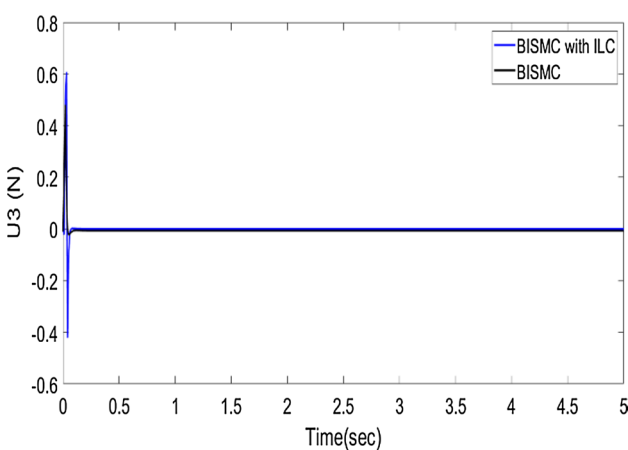


Fig. 11 Control input U_2 (N)

In addition, the controller parameters are selected as: $k_1 = 100, k_2 = 100, k_3 = 100, k_4 = 100, K, \epsilon, c_1, c_2, c_3, c_4 > 0$. The parameters of the Quadrotor UAVs dynamic were listed in Table 1.

It should be mentioned that the desired trajectory, the actual tracking by BISM with ILC, and the comparative method are shown in red, blue, and black.

The simulation results are shown in Figs. 4, 5, 6, 7, 8, 9, 10, 11, 12 and 13. The time responses for the position tracking of the Quadrotor UAVs for $x, y,$ and z axes in the two control strategies are shown in Figs. 4, 5 and 6 respectively. As can be seen from these Figures, the proposed controller method has better tracking performance from their perspective reference commands, higher accuracy, and fast transient responses in comparison with another method in the presence of the uncertainties and external disturbances. It can be concluded that the trajectories tracking errors for the mentioned method is fewer than the comparative method by using the iterative learning control. By this means that,

Table 2 Numerical index

Name of Index	BISMC with ILC	BISMC
$\int z_3^2 + u_1^2$	652.57	738.17
$\int z_4^2 + u_2^2$	0.0569	0.0507
$\int z_5^2 + u_3^2$	2.2904	1.1948
$\int z_6^2 + u_4^2$	3.2689	2.9965

ILC process uses from previous information's to improve tracking accuracy by calculating the total control signal.

The time responses of the roll, the pitch, and the yaw angles under the two control schemes are drawn in Figs. 7, 8 and 9. From this Figures, it's crystal clear that the BISMC with ILC has more accurate performance for tracking the desired commands in comparison with the BISMC despite the uncertainties and external disturbances. From Figs. 4, 5, 6, 7, 8 and 9, it can be concluded that the iterative learning control by calculating the unknown disturbance input U_d in each iteration can reject the disturbances and help to the proposed controller (BISMC) for better tracking performance.

Figures 9, 10, 11 and 12 show the results of the control inputs for the translational and the rotational subsystems. ILC uses unknown disturbance input U_d and U_{BISMC} ; therefor in some control signals more control efforts are observed. Based on researches, the results of control inputs are in the acceptable ranges. In order to justify the better tracking of the mentioned control strategy, numerical indexes are given in Table 2 which shows the integral of squared errors and the control signals as error of the position state with u_1 and integral of the squared rotational angles states with their control signals as u_2 , u_3 , and u_4 for the proposed method and the comparative method. From this Table, it can be seen that despite the more control efforts for the mentioned control strategy, the numerical indexes are almost in a same range.

6 Conclusion

In this paper, the combination of the back- stepping integral sliding mode control was designed and analyzed for the Quadrotor UAVs. The main aim of the proposed controller (BISMC) is to track the desired trajectories which were implemented by the guidance laws (10) and (11). For precise control, an iterative learning control algorithm in addition to the proposed controller (BISMC) implemented. The iterative learning control was updated by some simple formulas according to the previous experiments in the presence of the uncertainties and external disturbance. Next, the commands which were generated by the iterative learning control as unknown disturbance input U_d were added to the U_{BISMC} . The simulation results illustrated that the iterative learning control with (BISMC) can be much better than only

(BISMC) in term of accuracy and fast response and disturbance rejection.

References

- Nemati H, Bando M, Hokamoto S (2017) Chattering attenuation sliding mode approach for nonlinear systems. *Asian J Control* 19(4):1519–1531
- Yin C, Huang X, Chen Y, Dadras S, Zhong SM, Cheng Y (2017) Fractional-order exponential switching technique to enhance sliding mode control. *Appl Math Model* 44:705–726
- Zheng Z, Xia YQ, Fu MY (2011) Attitude stabilization of rigid spacecraft with finite-time convergence. *Int J Robust Nonlinear Control* 21:686–702
- Gao YB, Luo WS, Liu JX et al (2017) Integral sliding mode control design for nonlinear stochastic systems under imperfect quantization. *Sci China Inf Sci* 60:1–11
- Haddadi SJ, Emamagholi O, Javadi F, Fakhariyan A (2015) Attitude control and trajectory tracking of an autonomous miniature aerial vehicle. In: *AI & robotics (IRANOPEN)*, Qazvin, pp 1–6
- Lee D, Jin K, Shankar S (2009) Feedback linearization vs. adaptive sliding mode control for a Quadrotor helicopter. *Int J Control* 7(3):419–428
- Wang Y, Xia Y, Shen H, Zhou P (2017) SMC design for robust stabilization of nonlinear Markovian jump singular systems. *IEEE Trans Autom Control* 99:1–6
- Wang Y, Shen H, Karimi H, Duan D (2017) Dissipativity-based fuzzy integral sliding mode control of continuous-time t–s fuzzy systems. *IEEE Trans Fuzzy Syst* 99:1–6
- Tian BL, Yin LP, Wang H (2015) Finite-time reentry attitude control based on adaptive multivariable disturbance compensation. *IEEE Trans Ind Electron* 62:5889–5898
- Tian BL, Liu LH, Lu HC et al (2018) Multivariable finite time attitude control for quadrotor UAV: theory and experimentation. *IEEE Trans Ind Electron* 65:2567–2577
- Tian BL, Lu HC, Zuo ZY et al (2018) Multivariable finite-time output feedback trajectory tracking control of quadrotor helicopters. *Int J Robust Nonlinear Control* 28:281–295
- Tian BL, Fan WR, Su R et al (2015) Real-time trajectory and attitude coordination control for reusable launch vehicle in reentry phase. *IEEE Trans Ind Electron* 62:1639–1650
- Tian BL, Fan WR, Zong Q (2015) Integrated guidance and control for reusable launch vehicle in reentry phase. *Nonlinear Dyn* 80:397–412
- Emam M, Fakhariyan A (2016) Attitude tracking of quadrotor UAV via mixed H_2/H_∞ controller: a LMI based approach. In: *24th Mediterranean conference on control and automation (MED2016)*, Athens, pp 390–395
- Niroumand J, Fakhariyan A (2015) Trajectory tracking via adaptive nonlinear control approach for a quadrotor MAV. In: *IRANOPEN*
- Massaoudi Y, Dorsaf E, Gaubert JP, Mehdi D, Damak T (2016) Experimental implementation of new sliding mode control law applied to a DC–DC boost converter. *Asian J Control* 18(6):2221–2233
- Espinoza T, Dzul AE, Lozano R, Parada P (2014) Backstepping-sliding mode controllers applied to a fixed-wing UAV. *J Intell Robot Syst* 73(1–4):67–79
- Li J, Zhang D (2018) Back-stepping and sliding-mode techniques applied to distributed secondary control of islanded microgrids. *Asian J Control* 20(3):1288–1295

19. Khebbache H, Tadjine M (2013) Robust fuzzy backstepping sliding mode controllers for a Quadrotor unmanned aerial vehicle. *J Control Eng Appl Inf* 15(2):3–11
20. Li Y, Sun K, Tong S (2018) Observer-based adaptive fuzzy fault-tolerant optimal control for SISO nonlinear systems. *IEEE Trans Cybern* 99:1–13
21. Zhang X, Liu X, Li Y (2018) Direct adaptive fuzzy back-stepping control for stochastic nonlinear SISO systems with unmodeled dynamics. *Asian J Control* 20(2):839–855
22. Pounds PE, Bersak DR, Dollar AM (2012) Stability of small-scale UAV helicopters and quadrotors with added payload mass under PID control. *Auton Robot* 33:129–142
23. Javidi F, Fakharian A, Seyedsajadi MS (2013) Fuzzy integral backstepping control approach in attitude stabilization of a quadrotor UAV. In: 13th Iranian conference on fuzzy systems
24. Zou Y, Zheng ZW (2015) A robust adaptive RBFNN augmenting back-stepping control approach for a model-scaled helicopter. *IEEE Trans Control Syst Technol* 23:2344–2352
25. Dong J, Bin H (2019) Novel fuzzy PID-type iterative learning control for quadrotor UAV. *Sensors* 19(1):24
26. Chirarattananon P, Ma KY, Wood RJ (2016) Perching with a robotic insect using adaptive tracking control and iterative learning control. *Int J Robot Res* 35(10):1185–1206
27. Pipatpaibul PI, Ouyang PR (2013) Application of online iterative learning tracking control for quadrotor UAVs. In: *ISRN robotics*
28. Schoellig AP, Mueller FL, D'Andrea R (2012) Optimization-based iterative learning for precise quadcopter trajectory tracking. *Auton Robots* 33(1–2):103–127
29. Hock A, Schoellig AP (2016) Distributed iterative learning control for a team of quadrotors. In: *IEEE conference*, pp 4640–4646
30. Xu R, Ozguner U (2006) Sliding mode control of a quadrotor helicopter. In: *IEEE conference on decision and control*, San Diego, pp 4957–4962
31. Schöllig A, D'Andrea R (2009) Optimization-based iterative learning control for trajectory tracking. In: *European control conference (ECC)*, Budapest, pp 1505–1510

Publisher's Note Springer Nature remains neutral with regard to jurisdictional claims in published maps and institutional affiliations.



Davood Allahverdy received his B.S. and M.Sc. degree in Control Engineering from Islamic Azad University, Science and Research Branch, Iran in 2015 and 2018 respectively. His research interests include Nonlinear Control, Estimation, Modeling and Control of Robotic systems.



Ahmad Fakharian received his B.S. and M.Sc. degree in Control Engineering from University of Tehran, Iran in 1999 and 2002 respectively. He received his Ph.D. degree in control engineering from Tarbiat Modares University, Iran in 2010. Now, he is an associate professor at faculty of Electrical, Biomedical and Mechatronics Engineering of Islamic Azad University, Qazvin Branch. His research interests include Convex Optimization, Large Scale Systems modeling and Control, Microgrids Modeling and Control and Biologic Systems Modeling and Control. He was the recipient of a postdoctoral program award from Lulea University of Technology, Sweden in 2010. Now, he is a guest researcher in this university with some collaborating works in the field of control and optimization of complex and large scale systems especially with application in Smart Grids.



Mohammad Bagher Menhaj received the Ph.D. degree from Oklahoma State University (OSU), Stillwater, in 1992. Then, he became a Postdoctoral Fellow with OSU. In 1993, he joined Amirkabir University of Technology, Tehran, Iran. He is author and coauthor of more than 350 technical papers, and four books. Now, he is a full professor at department of electrical engineering of AmirKabir University of Technology. His main research interests are theory of computational intelligence, learning automata, adaptive filtering and their applications in control, power systems, image processing, pattern recognition, and communications.